

Characterization of Ag(I), Co(II) and Cu(II) removal process from aqueous solutions using dolomite powder

Ahad Ghaemi^{*†}, Meisam Torab-Mostaedi^{**}, Shahrokh Shahhosseini^{*}, and Mehdi Asadollahzadeh^{**}

^{*}Department of Chemical Engineering, Iran University of Science and Technology, P. O. Box 16765-163, Tehran, Iran

^{**}Nuclear Fuel Cycle Research School, Nuclear Science and Technology Research Institute, P. O. Box 14155-1339, Amirabad, Tehran, Iran

(Received 12 January 2012 • accepted 9 July 2012)

Abstract—Dolomite, a natural adsorbent, was used for removal of Ag(I), Cu(II) and Co(II) from aqueous solutions. Adsorption parameters including pH, temperature and contact time have been investigated to obtain adsorption mechanism. The results of experiments showed that adsorption of the metal ions increased by increasing pH values up to 5.5. The adsorption process was initially fast. Equilibrium isotherm data were analyzed using Langmuir, Freundlich and Dubinin-Radushkevich isotherm models. Maximum adsorption capacity of Ag(I), Cu(II) and Co(II) was 1.34, 1.63 and 2.84 mg/g at 20 °C, respectively. Kinetic models including Lagergren first-order and pseudo-second-order were used to test kinetic data. The results showed that pseudo-second-order has good agreement with experimental data. Thermodynamic parameters of the process were also investigated at different temperatures. The negative values of Gibbs free energy and enthalpy changes for Ag(I), Cu(II) and Co(II) indicated the spontaneous and exothermic nature of the adsorption process.

Key words: Dolomite, Ag(I), Cu(II), Co(II), Adsorption Isotherm

INTRODUCTION

Contamination of heavy metal ions in water supplies has increased over the last years as a result of over population and expansion of industrial activities. Metal ions pollution has a harmful effect on biological systems and does not undergo biodegradation. Therefore, the elimination of toxic metal ions from aqueous solutions is very important from environmental, economical and protection of public health points of view [1,2].

Several treatment technologies such as adsorption, solvent extraction, precipitation, membrane filtration and ion exchange have been developed to remove the metal ions from aqueous solutions. Among these techniques, adsorption is a more useful, feasible and practical method for metal ion removal than are other processes [3-8].

In the adsorption technique, different natural and synthetic adsorbents were used to remove metal ions [9-14]. Synthetic adsorbents such as activated carbon have been used widely in wastewater treatment applications throughout the world. In spite of their prolific use, synthetic adsorbents remain an expensive material, since higher the quality of these adsorbents, the greater their cost [15]. Therefore, this situation makes it no longer attractive to be widely used in small-scale industries because of cost inefficiency [16,17].

Due to the problems mentioned previously, research interest into the production of alternative adsorbents to replace the costly synthetic adsorbents has intensified in recent years. Attention has been focused on the various adsorbents which have metal-binding capacities and are able to remove unwanted heavy metal ions from contaminated water at low cost. Because of their low cost and local availability, natural materials are classified as low-cost adsorbents.

There are many different natural minerals such as perlite, zeolite, chitosan and clay or certain waste products from industrial operations such as fly ash, coal and oxides of minerals which have high adsorption capacity and can remove metal ions from effluents at reasonable costs [18-21].

On the other hand, natural sorbents are widely used in water and sewage purification, ammonia and heavy metal ion removal, ion exchange in radioactive wastewater treatment, removal of oil pollution from water and adsorption of other components from liquid and gaseous phases [22,23]. Clay minerals are considered very important adsorbents in natural water systems because of their high surface area combined with the structural and pH dependent charge developed on their surfaces. Low-cost adsorbents are still needed and these should be easily regenerated or disposed of without substantial environmental impact. A review of more than 70 natural and synthetic adsorbents and their potential uses for metal ions removal has been reported [24].

The aim this study was to investigate the adsorption potential of Iranian dolomite as a low-cost adsorbent in the removal of Ag(I), Cu(II) and Co(II) ions from aqueous solution. Adsorption experiments were performed at different conditions to determine the optimum parameter values for the maximum adsorption of Ag(I), Cu(II) and Co(II) ions from aqueous solutions. The Langmuir, Freundlich and Dubinin-Radushkevich (D-R) models were used to describe equilibrium isotherms. The adsorption mechanisms of Ag(I), Cu(II) and Co(II) onto dolomite were also evaluated in terms of kinetics and thermodynamics.

EXPERIMENTS

1. Adsorbent Characterization

The dolomite sample used in this study was supplied from Tabriz

[†]To whom correspondence should be addressed.
E-mail: aghaemi@iust.ac.ir

(Iran). The dolomite was ground and sieved on a series of test sieves and then it was directly used as adsorbent without any chemical

Table 1. Chemical composition of dolomite

Compound	Weight percentage (%)
CaO	74.26
MgO	21.42
Na ₂ O	1.26
Al ₂ O ₃	1.09
SO ₃	0.85
Sc ₂ O ₃	0.38
Fe ₂ O ₃	0.22
Zn	0.06
TiO ₂	0.06
MnO	0.04
Cu ₂ O	0.04
Loss on ignition	0.32

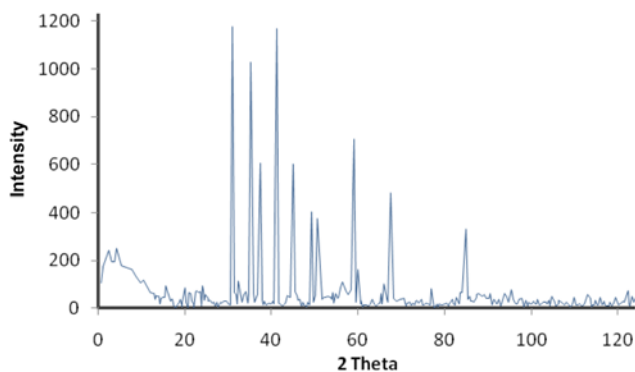


Fig. 1. XRD pattern of dolomite.

and thermal treatment, as this would be the most economical commercial product. The chemical composition of the dolomite used in these experiments was determined by X-ray diffraction (XRD) and it is summarized in Table 1. The structure of dolomite was detected by XRD scanning in 2 theta range of 0-120 and the obtained pattern was presented in Fig. 1. The specific surface area, average particle size and bulk density of dolomite are determined, respectively, as 1.82 m²/g, 20 μm and 2.83 g/cm³.

Dolomite is one of the many minerals that can be identified by FTIR, suggesting the technique might also be useful for identifying minerals associated with peaks in lithic fragments. FTIR spectra of minerals display characteristic features that can be related qualitatively to variations in the constituent minerals. Absorption features result from the detection of vibrational modes, i.e., lattice vibrations and/or molecular group vibrational modes. Qualitative mineral identification is possible because minerals have characteristic absorption bands in the midrange of the infrared, wave numbers 4,000 to 400 cm⁻¹. The typical diffuse reflectance FTIR spectrum of the dolomite is shown in Fig. 2.

The dolomite group is composed of minerals with an unusual trigonal bar 3 symmetry. The amount of calcium and magnesium in most specimens is equal, but occasionally one element may have a slightly greater presence than the other. Trace amounts of iron and manganese are sometimes also present [25].

Standards solutions of 1,000 ppm Ag(I), Cu(II) and Co(II) were prepared using analytical grade AgNO₃, CuCl₂ and Co(NO₃)₂, respectively. The sample solutions may be prepared from respective stock solutions.

2, Experimental Studies

Adsorption experiments were carried out using batch technique due to its simplicity and reliability. In the experiments 1.0 g of dolomite was agitated with 100 cm³ of the metal ion solution at 200 rpm in a mechanical shaker. The initial concentrations of Ag(I), Cu(II)

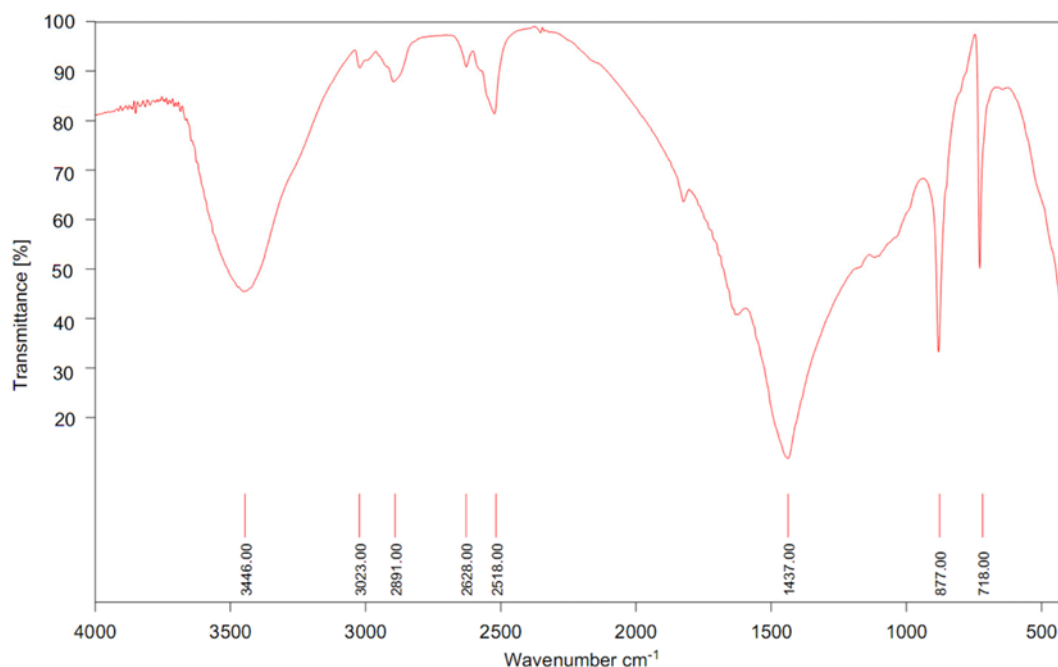


Fig. 2. FTIR spectra of dolomite, note that the absorption features at 3,445, 2,628 and 718 cm⁻¹ are characteristic of dolomite.

and Co(II) metal ions were 10, 20, 30, 40 and 50 ppm for studying the adsorption isotherm. The kinetic data were collected at 5, 10, 15, 30, 45, 60, 90, 120, 240 and 360 min to determine optimal contact time. To study the dependence of removal efficiency on pH, experiments were conducted in the pH range 2.5-8.5. The initial solution pH values were adjusted using 0.1 M HNO₃ or 0.1 M NaOH solution. The effect of temperature on the adsorption capacity of adsorbent was determined by using four different temperatures (20, 30, 40 and 50 °C). The aqueous samples were analyzed by using inductively coupled plasma-atomic emission spectroscopy (ICP-AES). The adsorption capacity of adsorbent was calculated through the following equation:

$$q_e = \frac{(C_i - C_e)V}{m} \quad (1)$$

Where q_e is the adsorption capacity (mg/g), C_i is the initial metal ion concentration (ppm), C_e is the equilibrium metal ion concentration in solution (ppm), m is the mass of adsorbent used (g) and V is the volume of the solution (L⁻¹). The adsorption percentage of metal ions was calculated as follows:

$$\text{Adsorption (\%)} = \frac{C_i - C_f}{C_i} \times 100 \quad (2)$$

Where C_i and C_f are the initial and final metal ion concentrations, respectively. The average absolute value of relative error, AARE, is used to compare the predicted results with the experimental data. This is defined as follows:

$$\text{AARE} = \frac{1}{N} \sum_{i=1}^N \left| \frac{\text{Predicted value} - \text{Experimental value}}{\text{Experimental value}} \right| \quad (3)$$

in which N is the number values of data points.

RESULTS AND DISCUSSION

1. Effect of pH

The pH parameter is one of the most important factors affecting the adsorption process [26]. The hydrolysis of metal ions is, in general, a function of both total metal ion concentration and pH. There are two distinct roles that concentration can play in the hydrolysis of metal ions: higher metal concentration lowers pH, thus repressing hydrolysis, and higher metal concentration increases the tendency to form polynuclear hydroxo complexes [27-29]. The effect of pH on the adsorption of Ag(I), Cu(II) and Co(II) onto dolomite was studied at pH 2.5-8.5.

As calcium oxide and magnesium oxide are the principal components of the adsorbent (Table 1), the differences between metal sorption capacities may be due to their affinity to the surface of them. The theoretical analysis of metal sorption on calcite surface is complex. It is well known that the adsorption of heavy metal ions by natural sorbents is dependent on pH, which extremely affects the ion exchange reactions and complexation as well physisorption processes [1].

The adsorption capacity of metal ions removed from solution versus pH is shown in Fig. 3. The adsorption of Ag(I), Cu(II) and Co(II) ions was highly dependent on the initial pH of heavy metal ions solution because pH influences the metal speciation and changes the charge in the adsorbent [27,28]. The pH experiments were carried

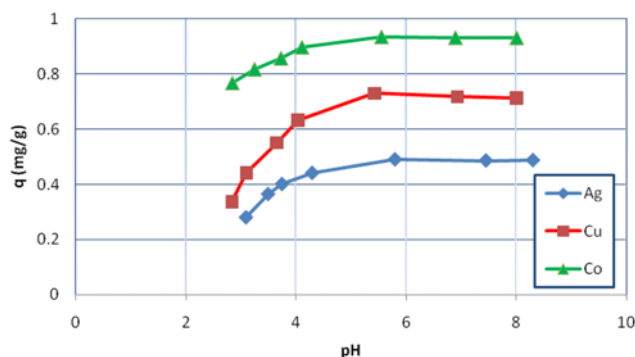
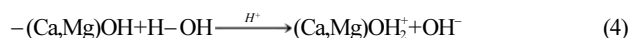


Fig. 3. Effect of pH on the adsorption of Ag(I), Cu(II) and Co(II) onto dolomite, $C[\text{Ag(I)}]_{\text{initial}}=10 \text{ mg/L}$, $C[\text{Cu(II)}]_{\text{initial}}=10 \text{ mg/L}$, $C[\text{Co(II)}]_{\text{initial}}=10 \text{ mg/L}$, $T=293 \text{ K}$, adsorbent concentration (m/V)=0.1 g/L, contact time $t=120 \text{ min}$.

out at metal ions concentration 10 ppm, adsorbent concentration 1.0 g·L⁻¹, temperature 293 °K and contact time 120 min.

At low pH values (pH<4), the low adsorption observation can be explained due to increase in positive charge density on the surface sites and, thus, electrostatic repulsion occurs between the metal ions and the edge group with positive charge (Ca,Mg-OH₂⁺) on the surface [25,30-32].



An increase in the adsorption occurred at pH 4-6 due to a decrease in positive charge density on dolomite surface sites, therefore decreasing the effect of electrostatic repulsion [18].



Where M^{2+} is metal ion (Ag(I), Cu(II) or Co(II)). The maximum Ag(I), Cu(II) and Co(II) adsorption was observed at pH 5.5. In the experiments, at higher pH values than 5.5, metal precipitation appeared and adsorbent deteriorated with accumulation of metal ions. Therefore, pH 5.5 was selected to be the optimum pH for further experimental studies.

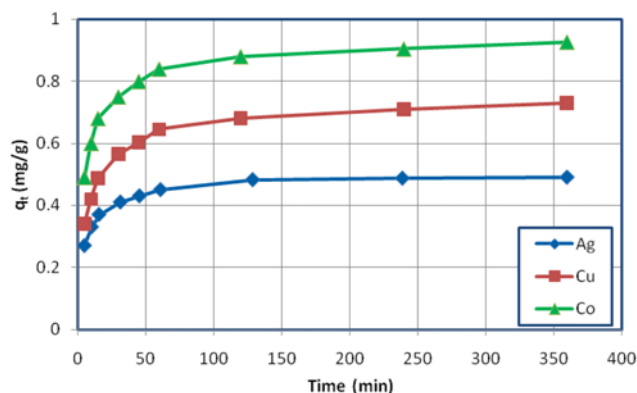


Fig. 4. Effect of contact time on the adsorption of Ag(I), Cu(II) and Co(II) ions by dolomite, $C[\text{Ag(I)}]_{\text{initial}}=10 \text{ mg/L}$, $C[\text{Cu(II)}]_{\text{initial}}=10 \text{ mg/L}$, $C[\text{Co(II)}]_{\text{initial}}=10 \text{ mg/L}$, $T=293 \text{ K}$, adsorbent concentration (m/V)=0.1 g/L, pH=5.5.

2. Adsorption Kinetics

To find the equilibrium time for the maximum uptake of Ag(I), Cu(II) and Co(II) on dolomite, the adsorption of the metal ions on dolomite was studied as a function of contact time. The results of kinetic data are shown in Fig. 4. As shown, the adsorption is very fast at initial contact time. The equilibrium was attained after shaking for 120 min. The adsorption kinetics were studied at pH 5.5, metal ions concentration 10 ppm, adsorbent concentration $1.0 \text{ g}\cdot\text{L}^{-1}$ and temperature 293 °K.

To investigate the mechanism of adsorption, kinetic models are generally used to test experimental data. Lagergren first order and Ho et al.'s pseudo-second-order rate equations were used to describe the kinetics of Ag(I), Cu(II) and Co(II) ions adsorption onto dolomite [13,33]. The first-order Lagergren rate equation used by researchers to study the kinetics of heavy metal ion adsorption is as follows:

$$\ln(q_e - q_t) = \ln q_e - k_1 t \quad (7)$$

Where q_t (mg/g) is the amount of the metal ions adsorbed at t (min) and k_1 is the rate constant of the adsorption (1/min). The values of k_1 and q_e can be calculated from the intercept and slope of the plots of $\ln(q_e - q_t)$ versus t .

The pseudo-second-order kinetic model equation is expressed as [33]:

$$\frac{dq}{dt} = k_2(q_e - q_t)^2 \quad (8)$$

Where k_2 is the rate constant of pseudo-second-order adsorption. For the same boundary conditions the integrated form becomes:

$$\frac{t}{q_t} = \frac{1}{k_2 q_e^2} + \frac{1}{q_e} t \quad (9)$$

If second-order kinetics is applicable, the plot of t/q against t should give a linear relationship, from which q_e and k_2 can be determined from the slope and intercept of the plot. Rate constants with model correlation coefficients and AARE values are given in Table 2. Figs. 5 and 6 show the nonlinear form of Lagergren first-order and pseudo-second-order for the adsorption of Ag(I), Cu(II) and Co(II), respectively. The results indicated that adsorption fitted well with the pseudo-

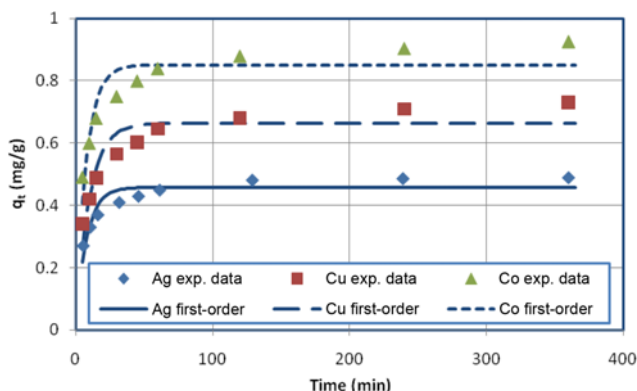


Fig. 5. First-order kinetic model for Ag(I), Cu(II) and Co(II) adsorption onto dolomite, $C[\text{Ag(I)}]_{\text{initial}}=10 \text{ mg/L}$, $C[\text{Co(II)}]_{\text{initial}}=10 \text{ mg/L}$, $C[\text{Cu(II)}]_{\text{initial}}=10 \text{ mg/L}$, $T=293 \text{ K}$, adsorbent concentration (m/V)=0.1 g/L, pH=5.5.

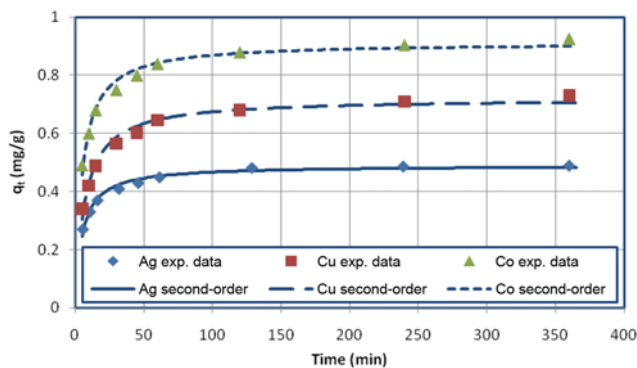


Fig. 6. Second-order kinetic model for Ag(I), Cu(II) and Co(II) adsorption onto dolomite, $C[\text{Ag(I)}]_{\text{initial}}=10 \text{ mg/L}$, $C[\text{Co(II)}]_{\text{initial}}=10 \text{ mg/L}$, $C[\text{Cu(II)}]_{\text{initial}}=10 \text{ mg/L}$, $T=293 \text{ K}$, adsorbent concentration (m/V)=0.1 g/L, pH=5.5.

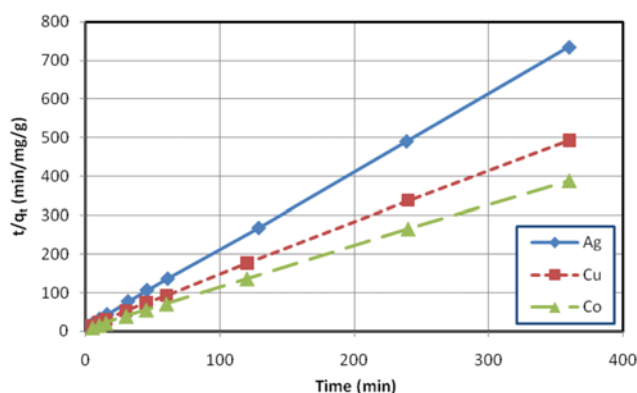


Fig. 7. The linear second-order kinetic sorption data for Ag(I), Cu(II) and Co(II) adsorption onto dolomite, $C[\text{Ag(I)}]_{\text{initial}}=10 \text{ mg/L}$, $C[\text{Co(II)}]_{\text{initial}}=10 \text{ mg/L}$, $C[\text{Cu(II)}]_{\text{initial}}=10 \text{ mg/L}$, $T=293 \text{ K}$, adsorbent concentration (m/V)=0.1 g/L, pH=5.5.

second-order kinetic model.

Fig. 7 shows Ho's linear plot of pseudo-second-order model for the kinetics of Ag(I), Cu(II) and Co(II) adsorption on dolomite. The kinetic parameters for the adsorption of Ag(I), Cu(II) and Co(II)

Table 2. Kinetic parameters for the adsorption of Ag(I), Cu(II) and Co(II) ions onto dolomite based on the first-order and pseudo-second-order models

Kinetic model	Ag(I)	Cu(II)	Co(II)
$q_{e(\text{exp.})}$ (mg/g)	0.49	0.73	0.927
Lagergren first order			
k_1 (min^{-1})	0.129	0.101	0.130
$q_{e(\text{cal.})}$ (mg/g)	0.458	0.664	0.851
R^2	0.838	0.855	0.837
AARE%	6.892	7.847	7.058
Pseudo-second order			
k_2 (g/mg min)	0.413	0.204	0.220
$q_{e(\text{cal.})}$ (mg/g)	0.489	0.720	0.912
R^2	0.983	0.980	0.979
AARE%	2.211	2.911	2.319

onto dolomite are summarized in Table 2. An analysis of the data in Table 2 indicates that the kinetics of adsorption of Ag(I), Cu(II) and Co(II) can be explained more accurately by the pseudo-second-order kinetic model. The values of correlation coefficient (R^2) and average absolute value of relative error (AARE) obtained for the pseudo-second-order kinetic model are better than that of Lagergren first-order kinetic model.

3. Adsorption Isotherm

The Langmuir isotherm applies to adsorption on completely homogeneous surfaces with negligible interaction between adsorbed molecules. The Langmuir model suggests monolayer sorption on a homogeneous surface without interaction between sorbed molecules. This model can be written in non-linear form as follows [34]:

$$\frac{C_e}{q_e} = \frac{1}{K_L q_m} + \frac{C_e}{q_m} \quad (10)$$

Where q_e is the amount of metal ion sorbed onto dolomite, K_L and q_m are Langmuir constants representing the equilibrium constant for the adsorbate-adsorbent equilibrium and the monolayer capacity. The Langmuir isotherm parameter was determined by least-squares fit of the sorption data. q_m and K_L were determined from the slope and intercept of the Langmuir linear form plot. The values of the parameters were presented at different temperature in Table 3. The isotherm experiments were carried out at pH 5.5, metal ion concentration 10 ppm, adsorbent concentration $1.0 \text{ g}\cdot\text{L}^{-1}$, temperature $293 \text{ }^\circ\text{K}$ and contact time 120 min.

The Freundlich isotherm model proposes a monolayer sorption with heterogeneous energetic distribution of active sites, accompanied by interactions between sorbed molecules. The Freundlich model is [35]:

$$\ln q_e = \ln k_f + n \ln C_e \quad (11)$$

Where k_f is a constant relating the sorption capacity and n is an empirical parameter relating the sorption intensity, which varies with

the heterogeneity. The values of Freundlich constants together with the correlation coefficients and AARE values at different temperatures are presented in Table 3.

Dubinin-Radushkevich does not assume an energetically homogeneous surface and proposes a nonhomogeneous distribution of adsorption sites. In particular, it assumes that the ionic species bind first with the most energetically favorable sites and that multilayer adsorption then occurs. The linear form of D-R isotherm model [36]:

$$\ln q_e = \ln q_m - \beta \varepsilon^2 \quad (12)$$

Where q_m is the theoretical saturation capacity, β is a constant related to the mean free energy of adsorption per mole of the adsorbate, β is the Polanyi potential ($=RT \ln(1+1/C_e)$), C_e is the equilibrium concentration of adsorbate in solution, R ($8.314 \text{ J}\cdot\text{mol}^{-1}\cdot\text{K}$) is the gas constant and T is the absolute temperature. The values of q_m and β were determined by plotting $\ln q_e$ versus ε^2 and presented in Table 3. The constant β gives an idea about the mean free energy E of adsorption per molecule of the adsorbate when it is transferred to the surface of the solid from infinity in the solution and can be calculated from the relationship [36]:

$$E = \frac{1}{\sqrt{2\beta}} \quad (13)$$

The magnitude of E is useful for estimating the type of adsorption process (physical or chemical). If the E value is between 8 and 16 kJ/mol, the adsorption process follows by chemisorption and if $E < 8$ kJ/mol, the process is a physisorption. Therefore, the results in Table 3 show that the adsorption of Ag(I), Cu(II) and Co(II) onto dolomite is a physisorption.

Figs. 8, 9 and 10 show the comparison of experimental data with the q_e values obtained by applying Langmuir, Freundlich and D-R models for adsorption of Ag(I), Cu(II) and Co(II), respectively. In the figures, it is clear that the experimental results fitted well with Langmuir model.

Table 3. Langmuir, Freundlich and D-R constants for adsorption of Ag(I), Cu(II), Co(II) on dolomite at different temperature

Isotherm models	293 ($^\circ\text{K}$)			308 ($^\circ\text{K}$)			323 ($^\circ\text{K}$)		
	Ag(I)	Cu(II)	Co(II)	Ag(I)	Cu(II)	Co(II)	Ag(I)	Cu(II)	Co(II)
Langmuir model									
K_L	0.104	0.272	0.694	0.063	0.176	0.414	0.021	0.076	0.214
q_m (mg/g)	1.342	1.629	2.842	0.749	1.142	2.187	0.519	0.967	1.326
R^2	0.993	0.985	0.997	0.984	0.995	0.979	0.952	0.976	0.995
AAER%	2.228	3.003	2.134	3.651	1.193	4.305	12.329	4.448	1.239
Freundlich model									
K_f	0.276	0.593	1.305	0.109	0.364	0.882	0.009	0.165	0.458
n	2.627	3.700	3.984	2.297	3.532	3.792	1.144	2.459	3.687
R^2	0.992	0.983	0.937	0.939	0.955	0.969	0.926	0.915	0.955
AAER%	2.470	3.189	9.494	7.321	4.529	5.034	12.54	8.580	4.631
D-R model									
β	2e-8	1e-8	1e-8	2e-8	2e-8	1e-8	4e-8	3e-8	1e-8
E (kJ/mol)	5.0	7.07	7.07	5.0	5.0	7.07	3.54	4.08	7.07
q_m (mg/g)	1.279	1.603	3.040	0.707	1.10	2.206	0.401	0.873	1.292
R^2	0.996	0.994	0.996	0.987	0.997	0.995	0.983	0.991	0.996
AAER%	7.145	3.828	3.044	8.22	7.20	1.678	6.032	6.47	8.502

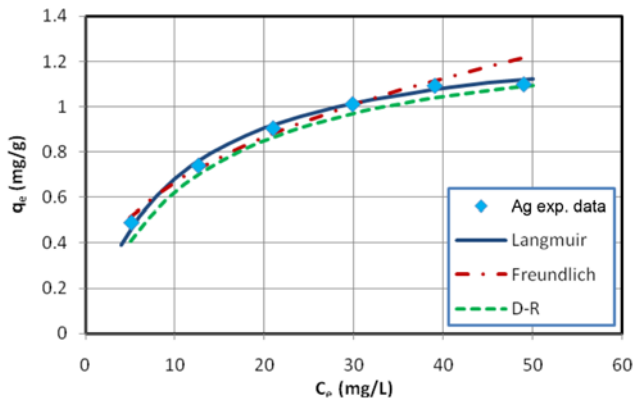


Fig. 8. Isotherm models of Ag(I) ion adsorption onto dolomite, $C[\text{Ag(I)}]_{\text{initial}}=10 \text{ mg/L}$, $T=293 \text{ K}$, adsorbent concentration (m/V)=0.1/L, pH=5.5, $t_{\text{contact}}=120 \text{ min}$.

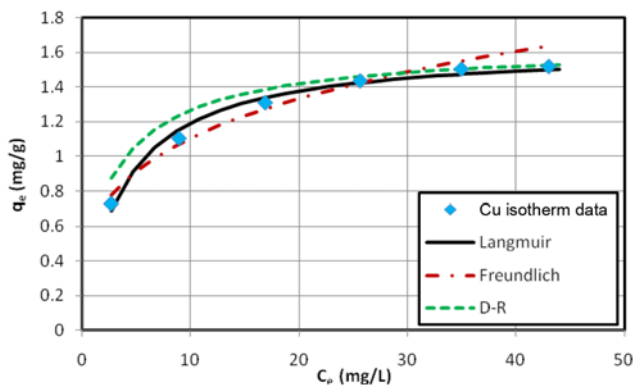


Fig. 9. Isotherm models of Cu(II) ion adsorption onto dolomite, $C[\text{Cu(II)}]_{\text{initial}}=10 \text{ mg/L}$, $T=293 \text{ K}$, adsorbent concentration (m/V)=0.1 g/L, pH=5.5, $t_{\text{contact}}=120 \text{ min}$.

The shape of the isotherm can also be considered when predicting whether an adsorption system is favorable or unfavorable. The essential characteristic of a Langmuir isotherm can be expressed in terms of a dimensionless separation factor or equilibrium parameter R_c , which is defined by the following equation [18]:

$$R_c = \frac{1}{1 + K_L C_e} \quad (14)$$

According to the value of R_c , the isotherm shape may be interpreted as given in Table 4. As shown in Table 5, the adsorption of Ag(I), Cu(II) and Co(II) ions onto dolomite is favorable.

A comprehensive coverage of different adsorbents under different environmental conditions can be found in the format of several

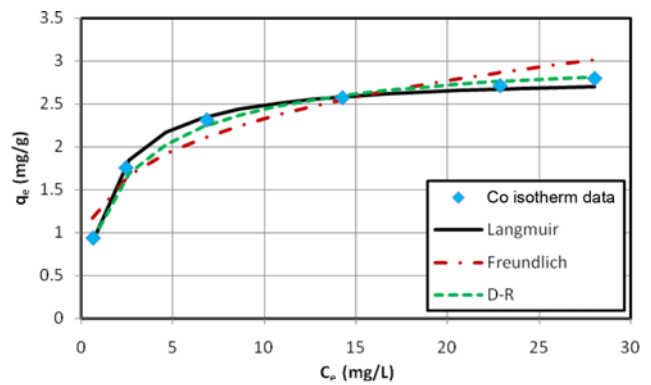


Fig. 10. Isotherm models of Co(II) ion adsorption onto dolomite, $C[\text{Co(II)}]_{\text{initial}}=10 \text{ mg/L}$, $T=293 \text{ K}$, adsorbent concentration (m/V)=0.1 g/L, pH=5.5, $t_{\text{contact}}=120 \text{ min}$.

Table 4. Separation factor for shape of isotherm

Value R_c	Type of adsorption
$R > 1.0$	Unfavorable
$R = 1.0$	Linear
$0 < R < 1.0$	Favorable
$R = 0$	Irreversible

Table 5. Dimensionless separation factor of Ag(I), Cu(II) and Co(II)

Metal ions	R_c		
	293 °K	308 °K	323 °K
Ag(I)	0.198-0.665	0.262-0.671	0.504-0.837
Cu(II)	0.095-0.577	0.124-0.545	0.235-0.654
Co(II)	0.059-0.689	0.076-0.641	0.109-0.542

publications. It may be seen that q_m values differ widely for different adsorbents. The adsorption capacity of different adsorbents for adsorption of Ag(I), Co(II) and Cu(II) are presented in Tables 6, 7 and 8 respectively. From Tables 6, 7 and 8, it can be concluded that dolomite exhibits moderate adsorption capacity toward Ag(I), Cu(II) and Co(II) ions. The fresh adsorbent price and the cost of regeneration/disposal of adsorbent are important issues that must be considered when selecting an adsorbent.

The comparison of the experimental adsorption capacity obtained in this study with the data in the literature for various adsorbents shows that dolomite is an effective sorbent of metal ions. These levels are similar to the achievable effluent levels of metal ions for a variety of wastewater treatment processes such as ion exchange and reverse

Table 6. Comparison of adsorption potential of various adsorbents for Ag(I) removal from aqueous solutions

Adsorbent	Ag(I) q_m (mg/g)	Ref.	Adsorbent	Ag(I) q_m (mg/g)	Ref.
Expanded perlite	8.46	[18]	Zeolite	33.2	[37]
Peat	10.8	[38]	Coke	4.9	[38]
Multisorb	36.1	[38]	Bituminous coal	6.4	[38]
Clinoptilolite	33.23	[40]	Low-rank Turkish coals	1.87	[39]
Dolomite	1.34	This work			

Table 7. Comparison of adsorption potential of various adsorbents for Co(II) removal from aqueous solutions

Adsorbent	Co(II) q_m (mg/g)	Ref.	Adsorbent	Co(II) q_m (mg/g)	Ref.
Hydroxyapatite nanoparticles	38	[1]	Bentonite	22.0	[9]
Activated carbon	13.9	[10]	Attapulgit	0.16	[11]
Lemon peel	22.0	[12]	Natural vermiculite	49.5	[40]
Kaolinite	0.92	[41]	Modified lignin	7.1	[42]
Soil	1.5	[43]	Marine bacterium	4.38	[44]
Nedalco sludge	11.71	[45]	Eerbeek sludge	12.34	[45]
Coir pith	14.07	[46]	Brown seaweed	20.63	[47]
MRA	35	[48]	Protonated alginate beads	35	[49]
Industrial waste and its cement fixation	35	[50]	Cross-linked calcium alginate beads	1.38	[51]
Dolomite	2.84	This work	Graphene oxide nanosheets	68.2	[27]

Table 8. Comparison of adsorption potential of various adsorbents for Cu(II) removal from aqueous solutions

Adsorbent	Cu(II) q_m (mg/g)	Ref.	Adsorbent	Cu(II) q_m (mg/g)	Ref.
Dolomite	8.26	[1]	Shells of lentil	9.59	[13]
Shells of rice	2.95	[13]	Shells of wheat	17.42	[13]
Expanded perlite	1.95	[18]	Peat	12.1	[16]
Composite chitosan biosorbent	86.2	[19]	Composite chitosan biosorbents	86.2	[19]
fired coal fly ash	20.92	[20]	Peat	6.2	[38]
Multisorb	8.3	[38]	Coke	3.1	[38]
Bituminous coal	1.37	[38]	Turkish bentonite	2.62	[52]
Clay	12.84	[53]	Unexpanded perlite	1.01	[54]
Unexpanded perlite	0.51	[54]	Expanded perlite	8.26	[55]
Expanded perlite	0.26	[56]	Low-rank Turkish coals	1.6	[57]
Red mud	5.3	[58]	Dye loaded sawdust	8.07	[59]
dye loaded groundnut shells	7.60	[59]	Tebengau (rice soil)	0.83	[60]
Idris (rice soil)	0.59	[60]	Anaerobically digested sludge	49.0	[61]
Chitosan flakes	20.9	[62]	Eutrophic peat	19.6	[63]
Treated <i>G. lucidum</i>	64.5	[64]	Amorphous iron hydroxide	14.0	[65]
Calcium-alginate	15.8	[66]	Sphagnum moss peat chitosan	16.8	[66]
Activated slag	35.3	[67]	Chitosan acetate crown ethers	31.3	[68]
Cross-linked chitosan	80.0	[69]	Grafted chitosan crown ether	41.3	[70]
Chitosan chelating resins	139.2	[71]	Chitosan-sulfonic acid resin	94.1	[72]
Chitosan	174.8	[73]	Amidoxime chitosan resin	153.2	[74]
Metal imprinted chitosan	56.5	[75]	Ether cross-linking chitosan	82.4	[75]
Beads of chitosan cross-linked with glutaraldehyde, epichlorohydrin and ethyleneglycol diglicidyl ether	59.6, 62.45, 45.9	[76]	Chitosan beads	80.7	[76]
			Multiwalled carbon nanotubes	6.19	[77]
			Nanostructured titanium oxide	52.63	[78]
			Dolomite	1.63	This work

Table 9. Thermodynamic parameters of Ag(I), Cu(II), Co(II) adsorption onto dolomite

Metal ion	ΔH° (kJ mol ⁻¹)	ΔS° (J mol ⁻¹ K ⁻¹)	ΔG° (kJ mol ⁻¹)			
			20 °C	30 °C	40 °C	50 °C
Ag	-41.90	-64.60	-22.97	-22.33	-21.68	-21.04
Cu	-33.25	-31.74	-23.95	-23.63	-23.31	-22.99
Co	-30.80	-16.57	-25.95	-25.78	-25.61	-25.45

osmosis. The sorbent used in this study has a number of constituents, the presence of which may explain the variation in the metal ion adsorptive capacities. In terms of electropositivity, conventional theory states that metal ions of lower electropositivity should adsorb

more readily.

4. Adsorption Thermodynamics

In the adsorption processes, energy and entropy factors must be considered in order to determine which process will occur sponta-

neously. From the variations of K_D with temperature, the integral heat of adsorption can be calculated using the van't Hoff equation [79]:

$$\ln K_D = \frac{\Delta S^\circ}{R} - \frac{\Delta H^\circ}{RT} \quad (15)$$

To investigate these parameters for our present system, adsorption kinetics were undertaken at 20, 30, 40 and 50 °C, from which the equilibrium constants, K_D , were evaluated. A plot of $\ln K_D$ as a function of $1/T$ is illustrated in Fig. 11. From this linear relationship, ΔH° and ΔS° can be calculated from the slope and intercept, respectively. Gibbs free energy (ΔG°) may be written in terms of entropy and enthalpy:

$$\Delta G^\circ = \Delta H^\circ - T\Delta S^\circ \quad (16)$$

The values of ΔG° , ΔH° and ΔS° are summarized in Table 9. The values of Gibbs free energy (ΔG°) can be calculated directly from Eq. (18). The ΔG° versus temperature is shown in Fig. 12. The negative ΔG° values indicate adsorption of Ag(I), Co(II) and Cu(II) are thermodynamically feasible and naturally spontaneous at 20-50 °C.

The negative value of the standard entropy, ΔS° , suggests decreased

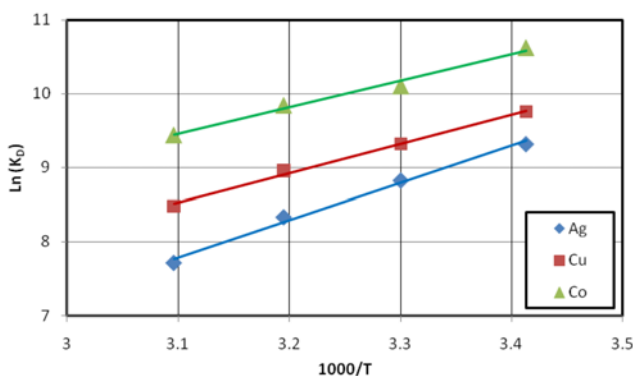


Fig. 11. $\ln K_D$ vs. $1/T$ for estimation of ΔH° and ΔS° , $T=20, 30, 40$ and 50 °C, $C[\text{Ag(I)}]_{\text{initial}}=10$ mg/L, $C[\text{Co(II)}]_{\text{initial}}=10$ mg/L, $C[\text{Cu(II)}]_{\text{initial}}=10$ mg/L, adsorbent concentration (m/V)=0.1 g/L, $\text{pH}=5.5$, $t_{\text{contact}}=120$ min.

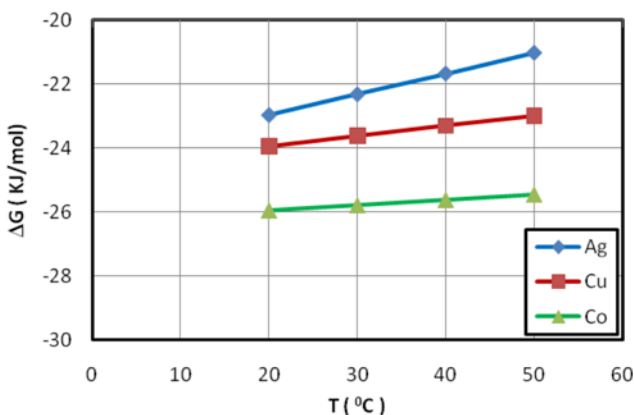


Fig. 12. Gibbs free energy (ΔG°) vs. temperature, $T=20, 30, 40$ and 50 °C, $C[\text{Ag(I)}]_{\text{initial}}=10$ mg/L, $C[\text{Co(II)}]_{\text{initial}}=10$ mg/L, $C[\text{Cu(II)}]_{\text{initial}}=10$ mg/L, adsorbent concentration (m/V)=0.1 g/L, $\text{pH}=5.5$, $t_{\text{contact}}=120$ min.

randomness at the solid/solution interface during the sorption Ag(I), Cu(II) and Co(II) ions onto dolomite. The change of the standard free energy increases with increase in temperature, which indicates that an increase in the temperature tended to decrease the adsorption capacity. The negative value of ΔH° again indicates the exothermic nature of the adsorption process. To summarize, these thermodynamic data indicate the adsorption process was exothermic.

CONCLUSION

The adsorption mechanism of Ag(I), Cu(II) and Co(II) onto dolomite was investigated both experimentally and theoretically. The adsorption was found to be dependent on pH, temperature and contact time. The optimum pH for the adsorption of the metal ions was found to be 5.5. The kinetic results indicated that the rate of adsorption of these metal ions was rapid and the data fitted well with the pseudo-second-order kinetic model. Also, equilibrium was attained after shaking for 120 min. Isotherm analysis of the data showed that the adsorption pattern of the metal ions onto dolomite followed the Langmuir model. Using the Langmuir model equation, the maximum capacity of dolomite was found to be 1.34, 1.63 and 2.84 mg/g for Ag(I), Cu(II) and Co(II) ions, respectively.

The values of separation factor (Table 5) for all ions showed that the adsorption of Ag(I), Co(II) and Cu(II) ions onto dolomite is favorable. Comparison of maximum adsorption capacity of dolomite with other adsorbent shows that dolomite exhibits moderate adsorption capacity toward Ag(I), Co(II) and Cu(II) ions. The experimental kinetic data were tested using kinetic models. The results showed that the pseudo-second-order rate equation best described the kinetic data of Ag(I), Co(II) and Cu(II) ions. Thermodynamic parameters depicted the exothermic nature of adsorption and the present adsorption processes were feasible and naturally spontaneous at 20-50 °C.

REFERENCES

1. E. Pehlivan, A. Mujdat, S. Dinc and S. Parlayici, *J. Hazard. Mater.*, **167**, 1044 (2009).
2. A. Imran and V. K. Gupta, *Nature London*, **1**, 2661 (2006).
3. K. S. Patel, K. Shrivastava, P. Hoffmann and N. Jakubowski, *Environ. Geochem. Health*, **28**, 11 (2006).
4. S. Kocaoba, *J. Hazard. Mater.*, **147**, 488 (2007).
5. J. Zeng, H. Ye and Z. Hu, *J. Hazard. Mater.*, **B161**, 1491 (2009).
6. E. Pehlivan and T. Altun, *J. Hazard. Mater.*, **B134**, 149 (2006).
7. M. Prasad, H. Xu and S. Saxena, *J. Hazard. Mater.*, **154**, 221 (2008).
8. K. Pagilla and L. W. Canter, *J. Environ. Eng.*, **125**, 243 (1999).
9. H. Omar, H. Arida and A. Daifullah, *Appl. Clay Sci.*, **44**, 21 (2009).
10. E. Demirba, *Adsorp. Sci. Technol.*, **21**, 951 (2003).
11. H. S. H. Chiu and J. J. Wang, *J. Environ. Protection Sci.*, **3**, 102 (2009).
12. A. Bhatnagar, A. K. Minocha and M. Sillanpää, *Biochem. Eng. J.*, **48**, 181 (2010).
13. H. Aydin, Y. Buluta and C. Yerlikaya, *J. Environ. Manage.*, **87**, 37 (2008).
14. H. Ghassabzadeh, M. Torab-Mostaedi, A. Mohaddespour and M. Ghannadi Maragheh, *Desalination*, **261**, 73 (2010).
15. W. Shen, Q. Guo, Y. Zhang, Y. Liu, J. Zheng, J. Cheng and J. Fan, *Physicochem. Eng. Aspects*, **273**, 147 (2006).

16. S. Babel and T. A. Kurniawan, *J. Hazard. Mater.*, **B97**, 219 (2003).
17. A. Imran, *Sep. Pur. Rev.*, **39**, 95 (2010).
18. H. Ghassabzadeh, A. Mohadespour, M. Torab-Mostaedi, P. Zaheri, M. Ghannadi Maragheh and H. Taheri, *J. Hazard. Mater.*, **177**, 950 (2010).
19. V. M. Boddu, K. Abburi, A. J. Randolph and E. D. Smith, *Sep. Sci. Technol.*, **43**, 1365 (2008).
20. A. Papandreou, C. J. Stourmaras and D. Papias, *J. Hazard. Mater.*, **148**, 538 (2007).
21. V. K. Gupta, *J. Environ. Manage.*, **90**, 2313 (2009).
22. P. Catalfamo, S. D. Pasquale, P. Primerano, L. Mavilia and F. Corigliano, *Mater. Eng. J.*, **7**, 67 (1996).
23. C. Colella, *Stud. Surf. Sci. Catal.*, **125**, 641 (1999).
24. S. E. Bailey, T. J. Olin, R. M. Brica and D. D. Adrin, *Water Res.*, **33**, 2469 (1999).
25. Y. Salameh, N. Al-Lagtah, M. N. M. Ahmad, S. J. Allen and G. M. Walker, *Chem. Eng. J.*, **160**, 440 (2010).
26. C. Chen and X. Wang, *Appl. Radiat. Isot.*, **65**, 155 (2007).
27. G. Zhao, J. Li, X. Ren, C. Chen and X. Wang, *Environ. Sci. Technol.*, **45**, 10454 (2011).
28. G. Sheng, Y. Shitong, J. Sheng, J. Hu, T. Xiaoli and W. Xiangke, *Environ. Sci. Technol.*, **45**, 7718 (2011).
29. S. Yang, J. Hu, C. Chen, D. Shao and X. Wang, *Environ. Sci. Technol.*, **45**, 3621 (2011).
30. K. O. Adebowale, I. E. Unuabonah and B. I. Olu-Owolabi, *J. Hazard. Mater.*, **B134**, 130 (2006).
31. A. Sari, M. Tuzen and M. Soylak, *J. Hazard. Mater.*, **B144**, 41 (2007).
32. G. M. Walker, J. A. Hanna and S. J. Allen, *Water Res.*, **39**, 2422 (2005).
33. Y. S. Ho and G. McKay, *Process Biochem.*, **34**, 451 (1999).
34. I. Langmuir, *J. Am. Chem. Soc.*, **40**, 1361 (1918).
35. H. M. F. Freundlich, *Zeitschrift für Physikalische Chemie (Leipzig)*, **57A**, 385 (1906).
36. M. M. Dubinin, E. D. Zaverina and L. V. Radushkevich, *Zhurnal Fizicheskoi Khimii*, **21**, 1351 (1947).
37. M. Akgul, A. Karabakan, O. Acar and Y. Yurum, *Micropor. Mesopor. Mater.*, **94**, 99 (2006).
38. P. Hanzlik, J. Jehlicka, Z. Weishauptova and O. Sebek, *Plant Soil Environ.*, **50**, 257 (2004).
39. A. Karabakan, S. Karabulut, A. Denizli and Y. Yurum, *Adsorpt. Sci. Technol.*, **22**, 135 (2004).
40. M. G. Fonseca, M. M. Oliveira, L. N. H. Arakaki, J. G. P. Espinola and C. Airoidi, *J. Colloid Interface Sci.*, **285**, 50 (2005).
41. O. Yavuz, Y. Altunkaynak and F. Güzel, *Water Res.*, **37**, 948 (2003).
42. A. Demirbas, *Energy Sources, Part A* **29**, 117 (2007).
43. J. P. Rawat, S. M. U. Iraqi and R. P. Singh, *Colloids Surf.*, **A 117**, 183 (1996).
44. A. Iyer, K. Mody and B. Jha, *Mar. Pollut. Bull.*, **50**, 340 (2005).
45. E. D. Van Hullebusch, A. Peerbolte, M. H. Zandvoort and P. N. L. Lens, *Chemosphere*, **58**, 493 (2005).
46. H. Parab, S. Joshi, M. Sudersanan, N. Shenoy, A. Lali and U. Sarma, *J. Environ. Sci. Health*, **A45**, 603 (2010).
47. K. Vijayaraghavan, J. Jegan, K. Palanivelu and M. Velan, *Sep. Purif. Technol.*, **44**, 53 (2005).
48. F. T. Awadalla and B. Pesic, *Hydrometallurgy*, **28**, 65 (1992).
49. J. P. Ibanez and Y. Umetsu, *Hydrometallurgy*, **64**, 89 (2002).
50. A. Bhatnagar, A. K. Minocha, B. H. Jeon and J. M. Park, *Sep. Sci. Technol.*, **42**, 1255 (2007).
51. T. Dewangan, A. Z. Tiwari and A. K. Bajpai, *J. Disp. Sci. Technol.*, **30**, 56 (2009).
52. G. Bereket, A. Z. Aroguz and M. Z. Ozel, *J. Colloid Interface Sci.*, **187**, 338 (1997).
53. O. Khazali, R. Abu-El-Halawa and Kh. Al-Souod, *J. Hazard. Mater.*, **B139**, 67 (2007).
54. M. Alkan and M. Dogan, *J. Colloid Interface Sci.*, **243**, 280 (2001).
55. A. Sari, M. Tuzen, D. Citak and M. Soylak, *J. Hazard. Mater.*, **148**, 387 (2007).
56. K. G. Bhattacharyya and S. S. Gupta, *Ind. Eng. Chem. Res.*, **45**, 7232 (2006).
57. S. Karabulut, A. Karabakan, A. Denizli and Y. Yurum, *Sep. Purif. Technol.*, **18**, 177 (2000).
58. H. Nadaroglu, E. Kalkan and N. Demir, *Desalination*, **9**, 138 (2009).
59. S. R. Shukla and R. S. Pai, *Sep. Purif. Technol.*, **43**, 1 (2005).
60. A. T. Choudhury and Y. M. Khanif, *Commun. Soil Sci. Plant Anal.*, **31**, 567 (2000).
61. M. S. Gould and E. J. Genetelli, *Water Res.*, **12**, 505 (1978).
62. R. Bassi, S. O. Prasher and B. K. Simpson, *Sep. Sci. Technol.*, **35**, 547 (2000).
63. X. H. Chen, T. Gosset and D. R. Thevenot, *Water Res.*, **24**, 1463 (1990).
64. C. N. R. Rao, L. Iyengar and C. Venkobachar, *J. Environ. Eng.*, **119**, 369 (1993).
65. S. Mustafa and I. Haq, *Environ. Technol. Lett.*, **9**, 1386 (1988).
66. C. Huang, Y. C. Chung and M. R. Liou, *J. Hazard. Mater.*, **45**, 265 (1996).
67. V. K. Gupta, *Ind. Eng. Chem. Res.*, **37**, 192 (1998).
68. S. Tan, Y. Wang, C. Peng and Y. Tang, *J. Appl. Polym. Sci.*, **71**, 2069 (1999).
69. R. Schmuhl, H. M. Krieg and K. Keizer, *Water SA*, **27**, 1 (2001).
70. Z. Yang, Y. Wang and Y. Tang, *J. Appl. Polym. Sci.*, **75**, 1255 (2000).
71. C. Ni and Y. Xu, *J. Appl. Polym. Sci.*, **59**, 499 (1996).
72. K. Kondo, S. I. Nakagawa, M. Matsumoto, T. Yamashita and I. Furukawa, *J. Chem. Eng. Japan*, **30**, 846 (1997).
73. R. S. Juang, F. C. Wu and R. L. Tseng, *Water Res.*, **33**, 2403 (1999).
74. K. Kondo, M. Matsumoto and K. Okamoto, *J. Chem. Eng. Japan*, **32**, 217 (1999).
75. T. Tianwei, H. Xiaojing and D. Weixia, *J. Chem. Technol. Biotechnol.*, **76**, 191 (2001).
76. W. S. Wan Ngah, A. Kamari and Y. J. Koav, *Int. J. Biol. Macromol.*, **34**, 155 (2004).
77. S. Debnath and U. Chand, *Desalination*, **273**, 330 (2011).
78. G. Sheng, J. Li, D. Shao, J. Hu, C. Chen, Y. Chen and X. Wang, *J. Hazard. Mater.*, **178**, 333 (2010).
79. Sh. Hasan, A. Krishnaiah, T. K. Ghosh and D. S. Viswanath, *Ind. Eng. Chem. Res.*, **45**, 5066 (2006).